

August 08, 2011

Magnetic signature of symmetry reduction in epitaxial $\text{La}_{0.67}\text{Sr}_{0.33}\text{MnO}_3$ films

Radhika Barua
Northeastern University

L. H. Lewis
Northeastern University

D. Heiman
Northeastern University

Recommended Citation

Barua, Radhika; Lewis, L. H.; and Heiman, D., "Magnetic signature of symmetry reduction in epitaxial $\text{La}_{0.67}\text{Sr}_{0.33}\text{MnO}_3$ films" (2011). *Physics Faculty Publications*. Paper 182. <http://hdl.handle.net/2047/d20001192>

Magnetic signature of symmetry reduction in epitaxial $\text{La}_{0.67}\text{Sr}_{0.33}\text{MnO}_3$ films

Radhika Barua,^{1,a)} L. H. Lewis,¹ and D. Heiman²

¹Department of Chemical Engineering, Northeastern University, Boston, Massachusetts 02115, USA

²Department of Physics, Northeastern University, Boston, Massachusetts 02115, USA

(Received 17 December 2010; accepted 18 July 2011; published online 8 August 2011)

The magnetic properties of epitaxially grown $\text{La}_{0.67}\text{Sr}_{0.33}\text{MnO}_3$ perovskite thin films were investigated to elucidate an unexpected broken symmetry between orthogonal [100] and [010] inplane directions, resulting from the magnetostructural coupling between the film and the cubic SrTiO_3 (001) substrate. The films were synthesized by molecular beam epitaxy with either complete or zero A-site cation disorder. Magnetization measured in [100] and [010] directions shows differences that signal a reduction of the in-plane cubic symmetry only for $T < 290$ K. The magnetization asymmetry is more robust in the film with complete A-site disorder. These results are attributed to a dominant Mn^{3+} character at the film-substrate interface and an associated out-of-plane bonding character with hypothesized origins in both charge imbalance and strain effects. © 2011 American Institute of Physics. [doi:10.1063/1.3623442]

Manganese-based $\text{La}_{1-x}\text{Sr}_x\text{MnO}_3$ (LSMO) compounds with the ABO_3 -type perovskite structure exhibit a profuse variety of structural, electronic, and magnetic phases.¹ $\text{La}_{0.67}\text{Sr}_{0.33}\text{MnO}_3$ is a metallic ferromagnet at room temperature² with unusual physical properties, such as colossal magnetoresistance (CMR)³ and almost total spin polarization (95% at 4 K)⁴ lending it significant potential for applications in spintronic devices. Bulk $\text{La}_{0.67}\text{Sr}_{0.33}\text{MnO}_3$ possesses a slightly distorted perovskite structure with a high Curie point $T_C = 370$ K and a saturation magnetization M_S of $3.7 \mu_B/\text{Mn}$.¹ In thin films, strain originating from lattice/substrate mismatch plays a fundamental role in defining the structural and electronic properties of $\text{La}_{0.67}\text{Sr}_{0.33}\text{MnO}_3$. The small lattice mismatch between LSMO and SrTiO_3 (STO) (0.83%) is favorable for the epitaxial growth of thin films of LSMO.⁵

Magnetic anisotropy can be an extremely sensitive probe of structural attributes in complex materials. While $\text{La}_{0.67}\text{Sr}_{0.33}\text{MnO}_3$ single crystals exhibit a uniaxial anisotropy in the (100) plane,⁶ films grown epitaxially on STO (001) develop an in-plane biaxial strain state with lower anisotropy in the orthogonal [100]/[010] directions relative to higher anisotropy in the [110] direction in the temperature range $20 \text{ K} \leq T \leq 300 \text{ K}$.^{7,8} Although the magnetocrystalline anisotropy energy of $\text{La}_{0.67}\text{Sr}_{0.33}\text{MnO}_3$ films has been widely studied as a function of temperature and film thickness,⁷⁻¹² very little work has been done on the magnetic response of films in the explicit [100]/[010] crystallographic directions. In addition, there has been very little work on the magnetic properties as a function of A-site disordering in epitaxial films. Thermodynamically synthesized $\text{La}_{1-x}\text{Sr}_x\text{MnO}_3$, characterized by random site population of La^{3+} and Sr^{2+} cations in the perovskite A lattice site, allows the B-site cations to exhibit a mixed $\text{Mn}^{3+}/\text{Mn}^{4+}$ valence state. Current state-of-the-art synthesis techniques such as ozone-assisted molecular beam epitaxy allow control of the A-site disorder by interleaving layers of LaMnO_3 (LMO) and SrMnO_3 (SMO) to create ordered artificial or “digitally layered” analogues of

$\text{La}_{1-x}\text{Sr}_x\text{MnO}_3$,¹³⁻¹⁵ represented as $[(\text{LMO})_{2n}(\text{SMO})_n]_m$, where n indicates the number of constituent integer layers and m refers to the number of repeating units. In this manner, the correlations between spin, charge, and orbital degrees of freedom at the layer interface may be systematically investigated for their potential to generate novel states of matter.

In the present study, we employ magnetic measurements to investigate an unexpected and persistent asymmetry in the temperature dependence of the magnetization along the orthogonal [100] and [010] in-plane directions of $\text{La}_{0.67}\text{Sr}_{0.33}\text{MnO}_3$. This asymmetry signals a reduction in the in-plane symmetry of the film below room temperature and challenges the general assumption in the literature that $\text{La}_{0.67}\text{Sr}_{0.33}\text{MnO}_3$ films retain in-plane cubic anisotropy at all temperatures. This phenomenon is observed in both the A-site-ordered and -disordered films, with a more robust effect evident in the disordered sample. This easy-plane uniaxial magnetic anisotropy is tentatively attributed to symmetry modifications along the in-plane directions [100] and [010] stemming from a dominant Mn^{3+} configuration and associated out-of-plane $d_{3z^2-r^2}$ bonding characterizing the LSMO-STO interface, as reported recently by Lee *et al.* with hypothesized origins in both charge imbalance and strain effects.¹⁶

Films of composition $\text{La}_{0.67}\text{Sr}_{0.33}\text{MnO}_3$ were epitaxially grown on STO (001) substrates with a low-angle vicinal cut of 0.22° using ozone-assisted molecular beam epitaxy. Details regarding the growth are reported elsewhere.^{14,15} The films possess a nominally tetragonal structure with $c/a < 1$ and are confirmed to be epitaxially strained in the basal (ab) plane to the STO substrate ($a_{\text{STO}} = 3.905 \text{ \AA}$). The nominal thicknesses, lattice parameters, and corresponding calculated strain values for the two film types at room temperature are reported in Table I. Bulk strain (ε_B) and biaxial strain (ε^*) values are calculated using the analytical model proposed by Millis *et al.*¹⁷ and indicate that both films exhibit small but finite stress. The difference in the thicknesses of the two films (A-site-ordered = 30 nm and A-site-disordered = 50 nm) leads to a difference in calculated bulk strain value ε_B , with the A-site-ordered film experiencing less bulk strain than the A-site disordered film. However, as

^{a)} Author to whom correspondence should be addressed. Electronic mail: barua.r@neu.edu.

TABLE I. Lattice parameters and corresponding strain values of the randomly alloyed film and the digitally synthesized superlattice of $\text{La}_{1-x}\text{Sr}_x\text{MnO}_3$ ($x = 0.33$). The bulk lattice parameter value of $a = 3.87\text{\AA}$ was used to calculate the strain.

	Lattice parameter (\AA) and strain (%)				
	Thickness (nm)	in-plane ($a = b$)	out-of-plane (c)	Bulk strain	Biaxial strain
Random Alloy ($\text{La}_{0.67}\text{Sr}_{0.33}\text{MnO}_3$)	50	3.90 (0.77)	3.84 (-0.78)	0.25	0.78
Digital superlattice $[(\text{LaMnO}_3)_2(\text{SrMnO}_3)]_{25}$	30	3.91 (1.02)	3.85 (-0.52)	0.51	0.77

shown in Table I, the ε^* values are the same for both films. These calculations imply that development of the in-plane magnetization should be the same for both films at room temperature.

A Quantum Design MPMS superconducting quantum interference device (SQUID) magnetometer was used for magnetic characterization of the LSMO films. The development of magnetization (M) as a function of temperature (T) in the range $10\text{ K} \leq T \leq 400\text{ K}$ at applied fields $H = 25, 50, 100,$ and 250 Oe was studied in the orthogonal in-plane crystallographic directions [100] and [010] in both zero-field-cooled (ZFC) and field-cooled (FC) conditions. The Curie temperature T_C was determined from the derivative of the M - T data as shown in Fig. 1 which confirms that the films develop a spontaneous magnetization at Curie temperatures that are suppressed from the bulk value of 370 K ,² where $T_C = 340\text{ K}$ for the random alloy film and $T_C = 320\text{ K}$ for the A-site ordered superlattice film.

At $T \sim 105\text{ K}$, STO undergoes a second-order phase transition from cubic to tetragonal symmetry ($c/a = 1.00056$).¹⁸ As observed by Ziese *et al.*,¹⁹ the STO structural transition at 105 K in magnetoelastically coupled STO/LSMO bilayers induces a magnetic perturbation in LSMO films which is manifest in the data of Fig. 1 by the magnetization dip $\sim 100\text{ K}$ that is observed only at low fields, $H \leq 100\text{ Oe}$. Fig. 2 displays the field-cooled magnetization trend $M(T)$ measured upon heating from 20 K for both the random alloy film, ($\text{La}_{0.67}\text{Sr}_{0.33}\text{MnO}_3$) and the digital superlattice film, $[(\text{LaMnO}_3)_2(\text{SrMnO}_3)]_{25}$ measured in the [100] and [010] directions. In both types of films, there is a difference in the magnitude of the magnetization along the two in-plane orthogonal directions until a critical temperature is reached (290 K for the random A-site film, Fig. 2(a) and 275 K for the A-site-ordered film, Fig. 2(b)), above

which the $M(T)$ curves superimpose. These trends are only observed at low fields: the $M(T)$ data converge completely at 50 Oe for the A-site ordered film, and at a much higher field of 250 Oe for the A-site-disordered film, indicating that the anisotropy field H_K in the [100] and [010] crystallographic directions is greater in the random alloy than in the A-site-ordered film. The hysteresis curves shown in Fig. 3 indicate that the in-plane anisotropy field H_K of the A-site-ordered film (200 Oe) is indeed smaller than that of the random alloy film (400 Oe) as demonstrated from the intersection of the [100] and [010] first-quadrant magnetization curves. In agreement with the anisotropy field observations, the measured coercivity H_c is somewhat smaller for the thinner A-site-ordered film ($H_c = 11\text{ Oe}$) than for the thicker A-site-disordered film ($H_c = 30\text{ Oe}$). This trend is opposite to typical observations, where a thicker ferromagnetic film often possesses a lower coercivity by virtue of the relative ease of reverse domain nucleation under the influence of a reversed field. It must be noted that finite differences in field-dependant magnetization in the orthogonal [100] and [010] directions have been reported in the heteroepitaxial system $\text{SrTiO}_3\text{-La}_{0.67}\text{Sr}_{0.33}\text{MnO}_3$ at low temperatures⁷ and in a thin 5 nm film.¹⁰

The observed low-temperature asymmetry in the LSMO in-plane film magnetization development is consistent with magnetic anisotropy differences originating from a crystallographic ordering or distortion lending an in-plane symmetry reduction that is sensitive to A-site order, magnetic field magnitude, and temperature. The reduction of in-plane film symmetry for $T < 275\text{ K}$ is tentatively attributed to an enhanced concentration of Mn^{3+} ions at the LSMO-STO interface, as deduced by Lee *et al.*¹⁶ using combined synchrotron and neutron probes. As the Mn^{3+} distribution in the epitaxial $\text{La}_{0.67}\text{Sr}_{0.33}\text{MnO}_3$ layer is not uniform along the

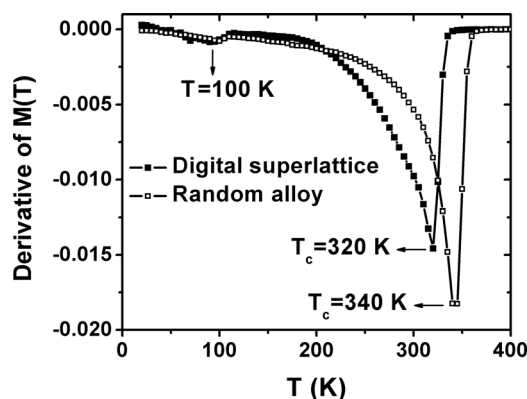


FIG. 1. Derivative of the temperature dependent magnetization, $M(T)$ as a function of temperature at $H = 100\text{ Oe}$ for A-site disordered random-alloy and A-site ordered superlattice of composition $\text{La}_{1-x}\text{Sr}_x\text{MnO}_3$ ($x = 0.33$) with magnetic field applied in the in-plane easy direction of magnetization.

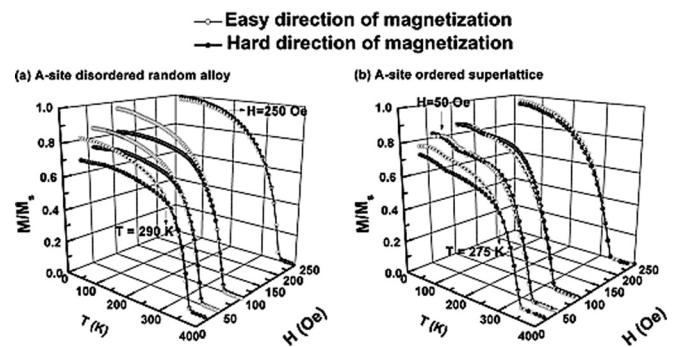


FIG. 2. Field-cooled temperature-dependent magnetization at $H = 25, 50, 100,$ and 250 Oe for A-site disordered random-alloy and A-site ordered superlattice of composition $\text{La}_{1-x}\text{Sr}_x\text{MnO}_3$ ($x = 0.33$) with magnetic field applied in the in-plane crystallographic directions [100] and [010]. The measured magnetization (M) is normalized to the saturation magnetization M_s as measured at 20 K . Arrows indicate applied field at which in-plane cubic anisotropy is restored.

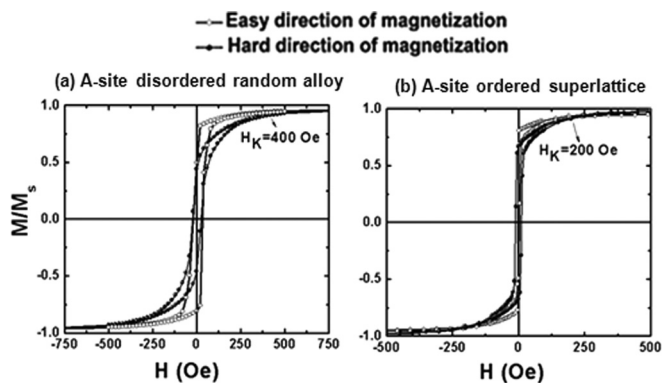


FIG. 3. Magnetic hysteresis loops measured at $T = 20$ K for A-site disordered random-alloy and A-site-ordered superlattice of composition $\text{La}_{1-x}\text{Sr}_x\text{MnO}_3$ ($x = 0.33$) with magnetic field applied in the in-plane crystallographic directions [100] and [010]. Arrows indicate anisotropy field H_K .

surface normal direction, the distribution of the orbital anisotropy in Mn^{3+} state relative to Mn^{4+} likewise is not uniform. Tensile strain that arises due to lattice mismatch between the film and the STO substrate favors $d_{x^2-y^2}$ orbital configuration at the interface.²⁰ However, owing to phase segregation of Mn^{3+} near the STO-film interface, $d_{3z^2-r^2}$ orbitals are energetically favored relative to the $d_{x^2-y^2}$ orbitals at the interface.^{21,22} The reconstructed $d_{3z^2-r^2}$ orbital configuration typically signals compressive strain in the $\text{La}_{0.67}\text{Sr}_{0.33}\text{MnO}_3$ lattice along the in-plane a, b axis.²⁰ It must be noted that during film synthesis, a single layer of SMO followed by a double layer of LMO was first deposited on the STO substrate. Given the rigorous conditions of the digital synthesis MBE deposition technique and the order of heterostructuring in the A-site ordered superlattice, in most likelihood the concentration of Mn^{3+} near the STO-film interface is smaller in the A-site-ordered superlattice than in the A-site-ordered random alloy. Thus, lowering of symmetry is less pronounced in the ordered superlattice.

Magnetization asymmetry along the orthogonal in-plane [100] and [010] directions may also be attributed to lattice modulations that help relieve stress originating from the strain mismatch between the LSMO and the underlying STO substrate.^{23,24} Biaxial lattice modulations aligned along [100] and [010] directions have been observed experimentally by Vigliante *et al.*²³ and Gebhardt *et al.*²⁴ in $\text{La}_{1-x}\text{Sr}_x\text{MnO}_3$ ($x = 0.1, 0.125$) films of nominal thickness $t \sim 50$ nm deposited on STO (001) substrates. It is also interesting to note similar conclusions reached in previous reports of asymmetric magnetic anisotropy measured along in-plane orthogonal directions authored by Krebs *et al.*²⁵ on single-crystal (001) Fe films deposited on GaAs substrates and by Chen *et al.*²⁶ on Co_2MnAl deposited epitaxially on GaAs. In all of these studies, the observed asymmetry in magnetic anisotropy is attributed to strain in the film-substrate interface that fosters inequivalence in the orthogonal bonding directions and lends a uniaxial anisotropy contribution to the existing cubic anisotropy.

In conclusion, we have established that epitaxial thin film samples of composition $\text{La}_{0.67}\text{Sr}_{0.33}\text{MnO}_3$ with thickness $t \leq 50$ nm deposited on single-crystal cubic SrTiO_3 (001) substrates show clear evidence of uniaxial in-plane

magnetic anisotropy in orthogonal directions below room temperature, a result which signals a reduction of in-plane cubic symmetry. The structural origin of the symmetry reduction remains unclear; however, future work aimed at structural characterization of $\text{La}_{0.67}\text{Sr}_{0.33}\text{MnO}_3$ thin-films using variable temperature x-ray diffraction (XRD) would be useful in confirming the presence of the hypothesized structural transition. These results add to our understanding of the fundamental magnetostructural properties of the heteroepitaxial material systems that are expected to play a key role in the development of future oxide-based nanodevice technologies.

Use of the Center for Nanoscale Materials was supported by the U.S. Department of Energy, Office of Science, Office of Basic Energy Sciences, under Contract No. DE-AC02-06CH11357. We acknowledge the support and intellectual input of Dr. Anand Bhattacharya and Dr. Tiffany Santos and Argonne National Laboratory for synthesis of the samples used in this study and for helpful discussions.

- ¹A. Urushibara, Y. Moritomo, T. Arima, A. Asamitsu, G. Kido, and Y. Tokura, *Phys. Rev. B* **51**, 14103 (1995).
- ²C. Zener, *Phys. Rev.* **82**, 403 (1951).
- ³S. Y. Yang, W. L. Kuang, C. H. Ho, W. S. Tse, M. T. Lin, S. F. Lee, Y. Liou, and Y. D. Yao, *J. Magn. Magn. Mater.* **226**, 690 (2001).
- ⁴M. Bowen, M. Bibes, A. Barthelemy, J.-P. Contour, A. Anane, Y. Lemaire, and A. Fert, *Appl. Phys. Lett.* **82**, 233 (2003).
- ⁵A. Hammouche, E. Siebert, and A. Hammou, *Mater. Res. Bull.* **24**, 367 (1989).
- ⁶Y. Suzuki, H. Y. Hwang, S. W. Cheong, T. Siegrist, R. B. van Dover, A. Asamitsu, and Y. Tokura, *J. Appl. Phys.* **83**, 7064 (1998).
- ⁷F. Tsui, M. C. Smoak, T. K. Nath, and C. B. Eom, *Appl. Phys. Lett.* **76**, 2421 (2000).
- ⁸K. Steenbeck and R. Hiergeist, *Appl. Phys. Lett.* **75**, 1778 (1999).
- ⁹M. Ziese, *Phys. Status Solidi B* **242**, R116 (2005).
- ¹⁰J.-L. Maurice, F. Pailloux, A. Barthelemy, O. Durand, D. Imhoff, R. Lyonnet, A. Rocher, and J.-P. Contoury, *Philos. Mag.* **83**, 3201 (2003).
- ¹¹L. M. Berndt, V. Balbarin, and Y. Suzuki, *Appl. Phys. Lett.* **77**, 2903 (2000).
- ¹²L. Ranno, A. Llobet, R. Tiron, and E. Favre-Nicolin, *Appl. Surf. Sci.* **188**, 170 (2002).
- ¹³A. Bhattacharya, X. Zhai, M. Warusawithana, J. N. Eckstein, and S. D. Bader, *Appl. Phys. Lett.* **90**, 222503 (2007).
- ¹⁴A. Bhattacharya, S. J. May, S. G. E. te Velthuis, M. Warusawithana, X. Zhai, B. Jiang, J.-M. Zuo, M. R. Fitzsimmons, S. D. Bader, and J. N. Eckstein, *Phys. Rev. Lett.* **100**, 257203 (2008).
- ¹⁵T. Santos, J. Steven, J. May, L. Robertson, and A. Bhattacharya, *Phys. Rev. B* **80**, 155114 (2009).
- ¹⁶J.-S. Lee, D. A. Arena, P. Yu, C. S. Nelson, R. Fan, C. J. Kinane, S. Langridge, M. D. Rossell, R. Ramesh, and C.-C. Kao, *Phys. Rev. Lett.* **105**(25), 257204 (2010).
- ¹⁷A. J. Millis, T. Darling, and A. Migliori, *J. Appl. Phys.* **83**, 1588 (1998).
- ¹⁸G. Shirane and Y. Yamada, *Phys. Rev.* **177**, 858 (1969).
- ¹⁹M. Ziese, I. Vrejoiu, A. Setzer, A. Lotnyk, and D. Hesse, *New J. Phys.* **10**, 063024 (2008).
- ²⁰Y. Tokura and N. Nagaosa, *Science* **288**, 462 (2000).
- ²¹A. Tebano, C. Aruta, P. G. Medaglia, F. Tozzi, G. Balestrino, A. A. Sidorenko, G. Allodi, R. De Renzi, G. Ghiringhelli, C. Dallera, L. Braicovich, and N. B. Brookes, *Phys. Rev. B* **74**, 245116 (2006).
- ²²C. Aruta, G. Ghiringhelli, A. Tebano, N. G. Boggio, N. B. Brookes, P. G. Medaglia, and G. Balestrino, *Phys. Rev. B* **73**, 235121 (2006).
- ²³A. Vigliante, U. Gebhardt, A. Rühm, P. Wochner, F. S. Razavi, and H. U. Habermeier, *Europhys. Lett.* **54**, 619 (2001).
- ²⁴U. Gebhardt, N. V. Kasper, A. Vigliante, P. Wochner, H. Dosch, F. S. Razavi, and H.-U. Habermeier, *Phys. Rev. Lett.* **98**, 096101 (2007).
- ²⁵J. J. Krebs, B. T. Jonker, and G. A. Prinz, *J. Appl. Phys.* **61**, 2596 (1987).
- ²⁶Y. J. Chen, D. Basiaga, J. R. O'Brien, and D. Heiman, *Appl. Phys. Lett.* **84**, 4301 (2004).